An unusual mechanism for EF-Tu activation during tmRNA-mediated ribosome rescue

MICKEY R. MILLER and ALLEN R. BUSKIRK[1]
Department of Chemistry and Biochemistry, Brigham Young University, Provo, Utah 84602, USA

ABSTRACT

In bacteria, ribosomes stalled on truncated mRNAs are rescued by transfer-messenger RNA (tmRNA) and its protein partner SmpB. Acting like tRNA, the aminoacyl-tmRNA/SmpB complex is delivered to the ribosomal A site by EF-Tu and accepts the transfer of the nascent polypeptide. Although SmpB binding within the decoding center is clearly critical for licensing tmRNA entry into the ribosome, it is not known how activation of EF-Tu occurs in the absence of a codon–anticodon interaction. A recent crystal structure revealed that SmpB residue His136 stacks on 16S rRNA nucleotide G530, a critical player in the canonical decoding mechanism. Here we use pre-steady-state kinetic methods to probe the role of this interaction in ribosome rescue. We find that although mutation of His136 does not reduce SmpB's affinity for the ribosomal A-site, it dramatically reduces the rate of GTP hydrolysis by EF-Tu. Surprisingly, the same mutation has little effect on the apparent rate of peptide-bond formation, suggesting that release of EF-Tu from the tmRNA/SmpB complex on the ribosome may occur prior to GTP hydrolysis. Consistent with this idea, we find that peptidyl transfer to tmRNA is relatively insensitive to the antibiotic kirromycin. Taken together, our studies provide a model for the initial stages of ribosomal rescue by tmRNA.

Keywords: tmRNA; SmpB; decoding; EF-Tu; ribosome

INTRODUCTION

In bacteria, translation of an mRNA lacking a stop codon leads to ribosome stalling at the 3′ end of the transcript. To rescue stalled ribosomes, bacteria make use of an RNA–protein complex consisting of transfer-messenger RNA (tmRNA) and its protein partner SmpB (for reviews, see Moore and Sauer 2007; Janssen and Hayes 2012). Acting as a tRNA, the tmRNA–SmpB complex enters the A-site of stalled ribosomes. Following transfer of the nascent peptide to Ala-tmRNA, the ribosome resumes translation using tmRNA as a template, adding an additional 10 amino acids that target the nascent peptide for proteolysis. At a stop codon, the tagged polypeptide is released, and the ribosomal subunits are recycled for additional rounds of translation. This process, known as *trans*-translation, tags about one out of every 200 proteins for degradation in exponentially growing *Escherichia coli* cells (Moore and Sauer 2005). tmRNA and SmpB are universally conserved in bacteria, are essential for growth in several species (Hutchison et al. 1999; Huang et al. 2000; Thibonnier et al. 2008), are required for pathogenesis in others (Julio et al. 2000; Okan et al. 2006), and have potential as novel antibiotic targets (Ramadoss et al. 2013).

A fundamental problem in understanding *trans*-translation is determining how the entry of tmRNA into the ribosomal A-site compares with the entry of aminoacyl-tRNAs. During canonical decoding, ribosomes discriminate between cognate and non-cognate aminoacyl-tRNAs through robust decoding mechanisms that ensure accurate translation of the genetic code (Zaher and Green 2009). Cognate tRNAs are selected through two kinetic discrimination steps that are separated by the hydrolysis of GTP by EF-Tu (Daviter et al. 2006). In the first step, cognate tRNAs trigger GTP activation at a faster rate than non-cognate tRNAs do (Pape et al. 1999; Gromadski and Rodnina 2004). The second selection step, or proofreading, occurs after GTP hydrolysis as the aminoacyl-tRNA is released from EF-Tu and undergoes full accommodation within the A-site. Cognate tRNAs are accommodated more rapidly than non-cognate tRNAs, which can be rejected prior to peptidyl transfer (Pape et al. 1999).

Cognate tRNAs achieve faster rates in these two selection steps through an induced-fit mechanism, as conformational changes in the ribosome occur in response to correct

[1]**Corresponding author**
E-mail buskirk@chem.byu.edu
Article published online ahead of print. Article and publication date are at http://www.rnajournal.org/cgi/doi/10.1261/rna.042226.113.

codon–anticodon pairing. At the local level, codon–anticodon pairing is monitored by conserved 16S nucleotides A1492 and A1493, which flip out of helix 44 and bind to the minor groove of the first and second base pairs in the codon–anticodon duplex. G530 also rotates from a *syn* to an *anti* conformation to interact with the second and third base pairs of the duplex (Ogle et al. 2001; Ogle and Ramakrishnan 2005; Schmeing et al. 2009). These local interactions are coupled to global conformational changes that effectively close the 30S subunit over the codon–anticodon helix (Ogle et al. 2002). Mutation of A1492, A1493, or G530 dramatically reduces the rates of EF-Tu activation and peptidyl transfer for cognate tRNAs, leading to lower fidelity in protein synthesis (Cochella et al. 2007).

The canonical decoding mechanism presents a challenge to our current understanding of *trans*-translation. During ribosome rescue, the decoding center interacts not with an RNA duplex but with tmRNA's protein partner SmpB. The tmRNA–SmpB complex mimics the shape of a canonical tRNA, with SmpB acting as the anticodon stem–loop (Bessho et al. 2007). Given that SmpB binding to the ribosomal decoding center protects A1492, A1493, and G530 from reacting with chemical probes (Nonin-Lecomte et al. 2009), we previously tested the model that SmpB's interaction with these key nucleotides might activate GTP hydrolysis through the canonical mechanisms described above. Arguing against this hypothesis, however, we found that mutation of A1492, A1493, and G530 had little or no effect on the rates of either GTPase activation or accommodation as tmRNA enters stalled ribosomes (Miller et al. 2011).

Reasoning that SmpB must play a key role in licensing tmRNA entry through some alternative mechanism, we also determined the role of several conserved residues in the C-terminal tail of SmpB (residues 133–160). Although we were unable to identify SmpB mutants that inhibit GTPase activation, we found that mutating key residues in the C-terminal tail prevents peptidyl transfer to tmRNA (Miller et al. 2011). Himeno and coworkers similarly reported that deletion of the tail abolishes peptidyl transfer but has no effect on GTPase activation (Kurita et al. 2010). In addition, they reported that high concentrations of a synthetic peptide corresponding to residues 133–160 blocks peptidyl transfer but not GTPase activation.

Here we revisit the question of EF-Tu activation by tmRNA and SmpB in light of the recent crystal structure of the *Thermus thermophilus* tmRNA–SmpB complex bound to the 70S ribosome (Neubauer et al. 2012). The structure reveals in detail how SmpB engages the decoding center. Helix 1 binds near A1492 and A1493, which are flipped out of helix 44 of the 16S rRNA, albeit in a conformation that is somewhat different from the conformation seen in canonical decoding (Fig. 1A). G530 stacks against the side chain of Tyr126, a conserved aromatic residue (His136 in *E. coli*). Conserved residues Lys128 and Arg129 bind to the sugar phosphate backbone of G530 and nucleotides nearby, perhaps stabilizing this stacking interaction (Fig. 1B). These structural findings prompted us to reevaluate the mechanism by which SmpB interacts with the decoding center to license entry of tmRNA into the A-site. In particular, we report biochemical evidence that the C-terminal tail plays a critical role in EF-Tu activation through a conserved base-stacking interaction with G530, as proposed by Ramakrishnan and coworkers (Neubauer et al. 2012). Contrary to previous reports (Kurita et al. 2010; Miller et al. 2011), our findings implicate the C-terminal tail in EF-Tu activation and further clarify the mechanism of how tmRNA enters stalled ribosomes.

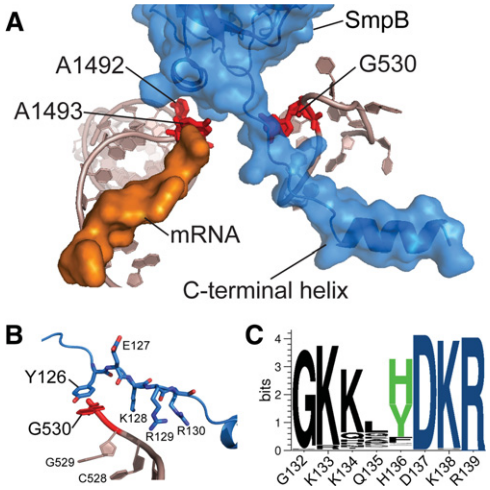

FIGURE 1. SmpB binding in the ribosomal decoding center. (*A*) SmpB (blue) engages 16S rRNA nucleotides A1492, A1493, and G530 (red). The C-terminal tail (residues 133–160) extends into the mRNA channel. Rendered using the *T. thermophilus* structures in PDB 4ABR (Neubauer et al. 2012). (*B*) Key SmpB residues interact with G530 and nearby nucleotides. Tyr126 corresponds to His136 in the *E. coli* protein. (*C*) Conserved residues in residues 132–139 are shown with the corresponding residues in *E. coli* SmpB listed below (Andersen et al. 2006).

RESULTS

The role of the SmpB C-terminal tail in EF-Tu activation

Although Himeno and coworkers reported that truncation of the C-terminal tail after residue 132 has no effect on GTP hydrolysis (Kurita et al. 2010), defects may have been overlooked. To test the importance of the SmpB tail using pre-steady-state kinetic methods, we assembled complexes composed of EF-Tu, GTP, Ala-tmRNA, and one of several SmpB variants. We also assembled initiation complexes containing an mRNA with a start codon in the P-site, Phe codon in the A-site, and no further downstream sequence. This mRNA construct allows us to react these initiation complexes with either the tmRNA–SmpB complex or Phe-tRNA as a control. GTP hydrolysis rates were measured by monitoring the appearance of inorganic phosphate over time as [γ-^{32}P]

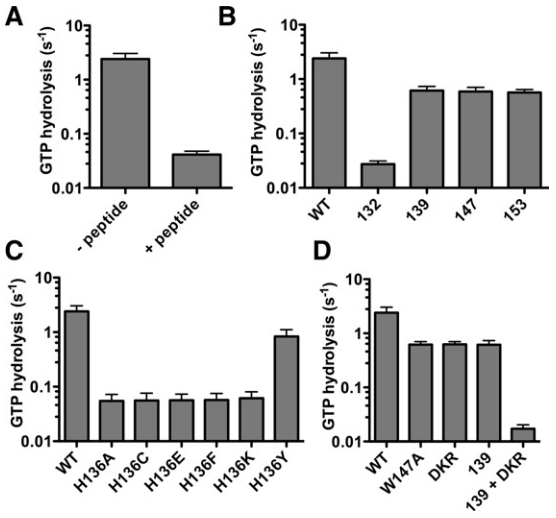

FIGURE 2. The SmpB C-terminal tail is critical for EF-Tu activation. GTP hydrolysis rates were measured by reacting complexes containing [γ-^{32}P]GTP, EF-Tu, SmpB, and Ala-tmRNA with 70S initiation complexes while monitoring the appearance of ^{32}P-labeled inorganic phosphate upon GTP hydrolysis. (*A*) The reaction was performed in the presence or absence of synthetic peptide corresponding to residues 133–160 of the SmpB tail. GTP hydrolysis rates were also obtained for a series of SmpB proteins: mutants truncated after the residue given (*B*), single amino acid changes at His136, the residue that stacks on G530 (*C*), and the D_{137}KR-to-AAA mutation and 139 truncation alone and in combination (*D*). The standard error is shown for the curve fit for the combination of two or more replicates.

GTP was hydrolyzed by EF-Tu. We note that the initiation complex concentration is not necessarily saturating in these reactions, and hence the observed rates may reflect changes in both binding and catalysis (k_{cat}/K_m). We found that addition of a synthetic peptide corresponding to tail residues 133–160 diminished the GTPase rate ~60-fold (Fig. 2A), presumably by competing with intact SmpB for the tail-binding site on the ribosome. We also found that deletion of the SmpB tail after residue 132 reduced the rate ~90-fold (Fig. 2B). In both cases, the loss of the interaction of the SmpB tail with the ribosome reduces GTPase activation rates, leading us to the conclusion that the C-terminal tail plays an essential role in EF-Tu activation, contrary to previous published models.

To pinpoint which residues in the SmpB tail induce EF-Tu activation, we created a series of SmpB truncation mutants and analyzed their GTP hydrolysis rates (Fig. 2B). In contrast to the dramatic, 90-fold reduction observed in the absence of the tail, truncation after residues 139, 147, or 153 resulted in only a modest, fourfold rate reduction. It appears that one or more residues between Gly132 and Arg139 are essential for activating EF-Tu. An analysis of the alignment of SmpB (Fig. 1C) shows several highly conserved residues in this region of the C-terminal tail. However, we previously showed that mutations of the conserved G_{132}K and D_{137}KR sequences had only a modest effect on GTP hydrolysis rates (Miller et al. 2011).

His136 in SmpB plays a role in EF-Tu activation

In the recent crystal structure of *T. thermophilus* tmRNA, SmpB, and EF-Tu bound to the ribosome (Neubauer et al. 2012), SmpB residue Tyr126 stacks with G530 of 16S rRNA. This residue is conserved as His or Tyr, both aromatic side chains capable of participating in base-stacking interactions. To test the importance of this interaction, we mutated the corresponding residue in *E. coli*, His136, to Ala and measured the rate of GTP hydrolysis by EF-Tu. This single mutation led to a 44-fold reduction in the rate of GTP hydrolysis (Fig. 2C). Similar defects were seen with the polar amino acids Cys, Lys, and Glu. Although a few species have the aromatic side chain Phe at this position, we found that the His136Phe mutation caused the same rate defect as His136Ala. In contrast, the His136Tyr mutation reduced the rate only threefold. The fact that the His136Tyr mutant is only modestly affected lends support to the structural finding that His136 interacts with the decoding center by stacking with the base of G530.

In a previous study (Miller et al. 2011), we showed that the G530A point mutation in 16S rRNA had no effect on EF-Tu activation by the tmRNA/SmpB complex. In an attempt to further disrupt the base-stacking interaction, we purified epitope-tagged ribosomes containing the G530U mutation since uracil stacks the poorest among the nucleobases (Rutledge et al. 2007). As expected, this ribosome mutation has a substantial effect on normal EF-Tu activation during canonical decoding with Phe-tRNA (Fig. 3). When reacted with the tmRNA–SmpB complex, however, the rate of GTP hydrolysis is not significantly reduced (only 1.3-fold). Nevertheless, we *do* see a synthetic effect when the His136Tyr SmpB variant is combined with G530U mutant ribosomes (about eightfold rate reduction). These synergistic effects are consistent with these two independent mutations affecting the same step in EF-Tu activation. Taken together, these findings support a model in which base stacking between His136 and G530 is essential for optimal GTP hydrolysis by EF-Tu in stalled ribosomes.

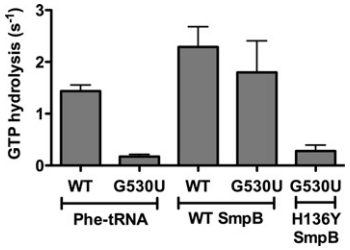

FIGURE 3. Synergistic effects between G530 and His136 mutants. GTP hydrolysis rates were measured for EF-Tu complexes containing either Phe-tRNA^{Phe} or Ala-tmRNA complexed with either wild-type or His136Tyr SmpB. These complexes were reacted with initiation complexes formed with tagged ribosomes that are either wild type or contain the G530U mutation.

Other residues in the SmpB tail play supporting roles in EF-Tu activation

The results from the 139, 147, and 153 truncation mutants suggest that other residues in the tail play at least a supporting role in EF-Tu activation. We hypothesized that additional interactions between the tail and the ribosome might help position His136 for stacking with G530. The C-terminal tail of SmpB forms an α-helix and binds in the mRNA channel of the ribosome (Miller et al. 2011; Neubauer et al. 2012). Within this channel, *T. thermophilus* SmpB residue Val137 forms hydrophobic interactions with the surface of ribosomal protein S5 (Neubauer et al. 2012). Himeno and coworkers reported that mutation of the corresponding residue in *E. coli* SmpB from Trp147 to Cys resulted in defects in peptidyl transfer but not EF-Tu activation (Kurita et al. 2010). We made the Trp147Ala mutant and observed that the GTP hydrolysis was diminished by fourfold (Fig. 2D). These effects are equivalent to those seen with truncations after 139.

In the *T. thermophilus* structure, two basic residues adjacent to Tyr126, Lys128, and Arg129 form ionic bonds with the sugar–phosphate backbone near G530 of 16S rRNA (Fig. 1B; Neubauer et al. 2012). Although these residues are highly conserved, we find that they play only a minor role in EF-Tu activation: Mutation of the corresponding *E. coli* residues D_{137}KR-to-AAA only has a fourfold effect (Fig. 2D). However, in the context of the 139 truncation, the DKR-to-AAA mutation decreases the rate of GTP hydrolysis more than 100-fold. This low level of activity is similar to what we observed in the 132 truncation mutant with the tail fully deleted. Perhaps Lys138 and Arg139 assist in EF-Tu activation, but their importance is masked by additional interactions between the ribosome and the residues in the SmpB tail after 139.

Mutations in the SmpB tail do not reduce ribosome-binding affinity

To test if the reduction in GTPase rates in the SmpB mutants results from impaired binding in the A-site, we used a fluorescence-binding assay to measure the affinity of SmpB for stalled ribosome complexes. By using SmpB alone, we were able to probe the SmpB–ribosome interaction directly without the added complications of tmRNA–ribosome binding and reactivity. Rodnina et al. (1996) have used aminoacylated tRNAs labeled with various fluorophores to monitor changes in tRNA structure in the ribosome. Structural changes produce altered fluorescence emissions as the environment of the fluorophore changes. Using $tRNA^{Phe}$ labeled with the fluorophore proflavine, we prepared ribosome complexes containing fMet-Phe-$tRNA^{Phe}$ bound in the P-site. To these complexes, we added wild-type SmpB, the 132 truncation mutant, or the His136Ala mutant, and monitored changes in fluorescence (Fig. 4A). From the fluorescence data, we calculated dissociation constants (K_d) for each of the SmpB proteins (Fig. 4B) and found that neither the 132-truncated SmpB nor the His136Ala mutant showed defects in binding to stalled ribosomes. These data agree with earlier reports (Sundermeier et al. 2005; Nonin-Lecomte et al. 2009) that the C-terminal tail is not required for high-affinity binding. These data support the conclusion that the His136 is not essential for ribosome binding per se but for promoting the activation of EF-Tu.

Release of tmRNA from EF-Tu is remarkably facile

Our data indicate that the C-terminal tail is essential for EF-Tu activation. In a previous study, we found that mutating conserved residues in the tail or blocking helix formation inhibits peptidyl transfer (Miller et al. 2011). To test the importance of His136 in this step, we reacted initiation complexes containing formyl-[^{35}S]Met-tRNA in the P-site with Ala-tmRNA and wild-type or His136Ala SmpB. Given that the His136Ala mutation leads to a 44-fold defect in the rate of EF-Tu activation, we expected a reduction in the rate of peptidyl transfer as well. Surprisingly, the rates were essentially equivalent for the wild-type and mutant SmpB (Fig. 5A), indicating that His136 is not essential for accommodation or peptidyl transfer. Although we cannot conclusively compare the rates of EF-Tu activation and peptidyl transfer, because the observed rates reflect k_{cat}/K_m under different reaction conditions, the fact that EF-Tu activation appears to be 25-fold slower than dipeptide formation led us to wonder if tmRNA were somehow being released from EF-Tu in a manner independent of GTP hydrolysis.

To probe the mechanism of tmRNA release from EF-Tu, we used the antibiotic kirromycin, which locks EF-Tu in its

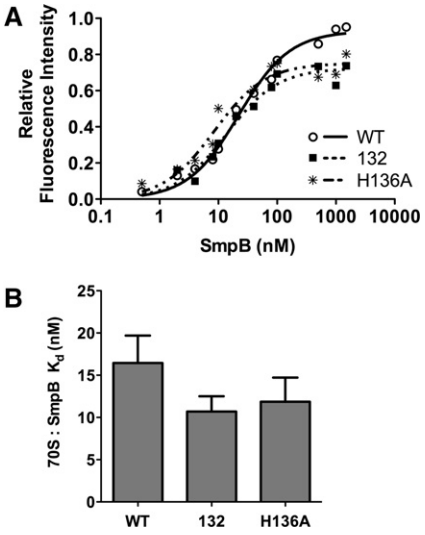

FIGURE 4. Binding of SmpB to stalled ribosome complexes. (*A*) Representative data showing the normalized fluorescence intensity of P-site bound, proflavine-labeled fMet-Phe-$tRNA^{Phe}$ upon SmpB binding. (*B*) Apparent dissociation constants were determined from the fluorescence data for wild-type SmpB and two SmpB tail mutants, one truncated after residue 132, the other containing the His136Ala point mutation. Each experiment was performed at least six times.

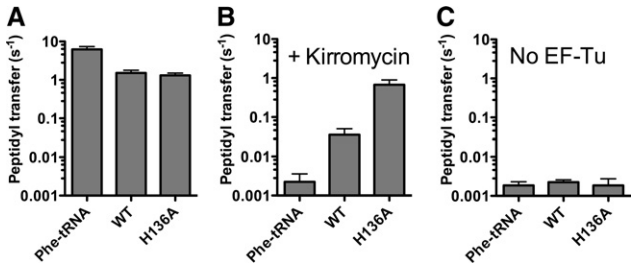

FIGURE 5. EF-Tu releases tmRNA more easily than Phe-tRNA prior to peptidyl transfer. Initiation complexes containing ^{35}S-labeled fMet-tRNA^{fMet} were reacted with the EF-Tu/Phe-tRNA complex or with the EF-Tu/Ala-tmRNA complex and either wild-type or His136Ala SmpB. Rates of dipeptide formation were determined in the absence (*A*) or presence (*B*) of 200 μM kirromycin, and in the absence of EF-Tu (*C*).

GTP-bound conformation, preventing release of aminoacylated tRNAs (Vogeley et al. 2001). As expected, in a control reaction, the rate of peptidyl transfer to Phe-tRNA^{Phe} was inhibited more than 1000-fold in the presence of kirromycin (Fig. 5, cf. A and B). However, when EF-Tu complexed with tmRNA and wild-type SmpB was reacted in the presence of kirromycin, the rate of peptidyl transfer was only reduced by ~40-fold. When the His136Ala mutant was used, kirromycin only reduced the rate of peptidyl transfer twofold (Fig. 5B). The release of tmRNA from EF-Tu occurs in a manner that is remarkably resistant to kirromycin, suggesting that tmRNA can be released for accommodation more easily than canonical tRNAs.

These surprising findings raise questions about the role of EF-Tu in *trans*-translation. Although EF-Tu binds tmRNA (Barends et al. 2001; Valle et al. 2003; Neubauer et al. 2012), there are also reports that peptidyl transfer to tmRNA occurs robustly even in the absence of EF-Tu (Hallier et al. 2004; Shimizu and Ueda 2006). To further test the role of EF-Tu in this process, we determined the rate of peptidyl transfer to Ala-tmRNA with and without EF-Tu. We found that peptidyl transfer occurs in the absence of EF-Tu, as reported (Hallier et al. 2004; Shimizu and Ueda 2006), but that the rate is ~1000-fold faster when EF-Tu is present (Fig. 5, cf. A and C). EF-Tu accelerates peptidyl transfer to Phe-tRNA by a similar amount. We conclude that EF-Tu dramatically accelerates peptidyl transfer to the tmRNA–SmpB complex, presumably by delivering the complex to the ribosomal A-site as occurs with canonical aminoacyl-tRNAs.

DISCUSSION

Stalled ribosomes accept Ala-tmRNA into the A-site in the absence of a codon–anticodon interaction. Structural and biochemical studies indicate that tmRNA's protein partner SmpB binds the decoding center in the 30S A-site (Kaur et al. 2006; Kurita et al. 2007; Nonin-Lecomte et al. 2009; Neubauer et al. 2012). Although the C-terminal tail of SmpB is essential for peptidyl transfer to tmRNA (Sundermeier et al. 2005; Kurita et al. 2010; Miller et al. 2011), it was not thought to play a role in EF-Tu activation. In the present study, we use pre-steady-state kinetic methods to clarify the role of the SmpB tail in licensing tmRNA entry into stalled ribosomes, showing that it is critical for both EF-Tu activation and peptidyl transfer.

In the crystal structure of *T. thermophilus* EF-Tu, SmpB, and tmRNA bound to the 70S ribosome and trapped in the A/T state, conserved residues in SmpB bind near A1492, A1493, and G530 in the decoding center. Mutation of positively charged residues in SmpB helix 1 (data not shown) or mutation of A1492 or A1493 had no significant effect on SmpB activity (Miller et al. 2011). These results are consistent with the fact that residues in helix 1 are not in close contact with the bases of A1492 and A1493. It seems unlikely that these interactions are essential for SmpB function.

Here we report kinetic data that provide biochemical evidence to support the structural observations of Ramakrishnan and coworkers that the His136 side chain stacks on the G530 base (Neubauer et al. 2012). His136 mutants that are incapable of stacking have dramatically lower GTP hydrolysis rates, indicating that this interaction is essential for EF-Tu activation. These findings help explain why residue 136 is conserved as His or Tyr, two residues with high base-stacking propensities. Notably, although the aromatic Phe side chain is capable of participating in base-stacking interactions, the His136Phe mutant is inactive. This loss of activity may be due to lower stacking energy, as nucleobases stack more poorly with Phe than with His or Tyr (Rutledge et al. 2007). Importantly, mutation of His136 to Ala or deletion of the C-terminal tail after residue 132 does not affect the affinity of SmpB for the ribosomal A-site. Although the tail apparently contributes little to overall SmpB binding energy, we speculate that His136 alters the conformation of G530, leading to conformational changes in the ribosome similar to those observed in the canonical decoding process. Indeed, the *T. thermophilus* structure shows that the tmRNA–SmpB complex induces closure of the 30S subunit as observed in canonical decoding (Neubauer et al. 2012).

In a previous study, we found that ribosomes containing the 16S rRNA mutation G530A supported rapid rates of peptidyl transfer and GTP hydrolysis by EF-Tu (Miller et al. 2011). Given that His136's interaction with G530 is through base stacking, it may be that G530A ribosomes do not exhibit significant rate defects because the stacking energies of His with guanine or adenine are similar (Rutledge et al. 2007). As the stacking energy between His and uracil is predicted to be substantially weaker, one might expect more of a reduction in the GTP hydrolysis rate in the G530U mutant than we observed. Indeed, in the presence of the His136Tyr SmpB mutant, the activity of the G530U ribosomes was substantially reduced. This synergistic defect is consistent with a mechanism in which both mutations (G530U and His136Tyr) cause defects at the same step. We speculate that GTPase activation is robust because binding and positioning of G530 and

His136 are aided both by the nearby residues Lys138 and Arg139 in the D_{137}KR sequence and by the interaction of the downstream portion of the C-terminal tail with the mRNA channel.

While activation of EF-Tu during *trans*-translation shares some mechanistic similarities to canonical translation, particularly the involvement of G530, we also observe some surprising differences. It appears that the tmRNA–SmpB complex may be more easily released from EF-Tu than canonical tRNAs are. The His136Ala SmpB mutation reduces the rate of EF-Tu activation such that it is 25-fold slower than the rate of peptidyl transfer, implying that peptidyl transfer may occur without GTP hydrolysis. Because our observed rates reflect k_{cat}/K_m, we cannot state this conclusively. However, the fluorescence binding assays and the lack of a peptidyl-transfer defect suggest that the His136Ala mutation has little or no effect on SmpB's ability to bind the ribosome. We speculate that this mutation primarily affects k_{cat} for GTP hydrolysis and that it does not affect peptidyl transfer because tmRNA can be released from EF-Tu even without GTP hydrolysis.

Consistent with this interpretation, we find that peptidyl transfer to tmRNA is unusually resistant to the antibiotic kirromycin. Kirromycin binds EF-Tu and blocks conformational changes after GTP hydrolysis, trapping aminoacyl-tRNAs onto EF-Tu (Vogeley et al. 2001). Kirromycin has only a modest effect on peptidyl transfer to tmRNA with wild-type SmpB and has essentially no effect with the His136Ala mutant. It appears that the tmRNA–SmpB complex is released from EF-Tu without the canonical conformational changes that result from GTP hydrolysis. The fact that EF-Tu binds to Ala-tmRNA more weakly than it binds Ala-tRNA (Barends et al. 2000, 2001) potentially contributes to facile tmRNA release from EF-Tu into the A-site. In support of this idea, we note that a mutation in EF-Tu that lowers its affinity for otherwise tight-binding aminoacyl-tRNAs increases the peptidyl-transfer rate because release from EF-Tu occurs more rapidly in the A-site (Schrader et al. 2011).

Contacts between the large tmRNA molecule and the ribosome may also partially explain its release from EF-Tu in the A-site. Ueda and coworkers found that peptidyl-transfer end points were unaffected by kirromycin (Shimizu and Ueda 2006). In contrast, peptidyl transfer to a truncated tmRNA containing only the tRNA-like domain (TLD) was blocked by kirromycin. These results raise the possibility that the body of tmRNA, consisting of four pseudoknots and the mRNA-like region, is at least partially responsible for tmRNA's unusual ability to undergo peptidyl transfer in the presence of kirromycin.

In general terms, it makes biological sense that EF-Tu activation is more important for canonical elongation than *trans*-translation because a different type of selectivity is involved. In canonical translation, the ribosome must select cognate aminoacyl-tRNAs; translational fidelity arises from two reversible tRNA selection steps separated by the irreversibility of GTP hydrolysis. In contrast, *trans*-translation does not require this same kind of substrate selectivity. Instead, *trans*-translation requires that tmRNA react selectively with stalled ribosomes and not actively translating ribosomes. tmRNA does not undergo rapid accommodation and peptidyl transfer if the mRNA extends more than 12–15 nucleotides (nt) after the P-site codon (Ivanova et al. 2004) because the SmpB tail cannot properly engage the mRNA channel (Neubauer et al. 2012). In *trans*-translation, although GTP hydrolysis may occur as EF-Tu delivers the tmRNA-SmpB complex, this event is probably not providing two opportunities for selectivity in the same way it does in canonical translation.

In conclusion, our data support the following model of the initial steps of *trans*-translation: EF-Tu delivers SmpB and Ala-tmRNA to the ribosomal A-site. The body of SmpB is responsible for its binding affinity in the decoding center. His136 stacks on G530 as positioned by D_{137}KR and other downstream tail residues. GTP is hydrolyzed and tmRNA is released from EF-Tu, although it is not clear that GTP hydrolysis is necessary for this release. If the C-terminal tail can enter the mRNA channel, the tmRNA–SmpB complex is accommodated fully into the A-site, and peptidyl transfer takes place. If the mRNA length downstream from the A-site codon is prohibitively long (12 nt or more), then the tmRNA–SmpB complex cannot accommodate properly and dissociates from the ribosome.

MATERIALS AND METHODS

Purification of translation components

Wild-type and G530U MS2-tagged ribosomes were expressed and purified as described (Youngman and Green 2005; Cochella et al. 2007; Miller et al. 2011). IF1, IF2, IF3, and His-tagged EF-Tu, PheRS, and AlaRS were purified as described (Shimizu et al. 2001; Cochella and Green 2005; Brunelle et al. 2006). Wild-type and mutant SmpB proteins were expressed and purified as described (Miller et al. 2011). Formyl-[^{35}S]Met-tRNA^{fMet} was prepared as described (Walker and Fredrick 2008). The mRNA GGAAUUCGGGCCC UUGUUAACAAUUAAGGAGGUAUACUAUGUUC was synthesized by T7 transcription of a template assembled by annealing sense and antisense oligonucleotides. It has a Phe codon in the A-site with nothing downstream so that when incorporated into initiation complexes, it can react with either tmRNA-SmpB or Phe-tRNA. tmRNA was synthesized and aminoacylated as described (Miller et al. 2011). The extent of tmRNA aminoacylation was 50%–60% as determined by a small parallel reaction with [^{14}C]-alanine. tRNA^{Phe} (Sigma-Aldrich) was aminoacylated with purified PheRS.

GTP hydrolysis reactions

70S initiation complexes and ternary and tmRNA-SmpB quaternary complexes were formed essentially as described (Miller et al. 2011). Initiation complexes were diluted to 400 nM prior to storage at −80°C. GTP hydrolysis rate reactions were carried out on a

KinTek RQF-3 quench-flow instrument at 20°C. Equal volumes of initiation complexes and either ternary or quaternary complexes were rapidly mixed and quenched with 40% formic acid at the desired times. Inhibition by the synthetic peptide corresponding to the C-terminal tail (133–160) of SmpB was performed by incubating 500 μM synthetic peptide with the initiation complex before mixing with quaternary complex. Reaction products were resolved on PEI cellulose TLC plates in 0.5 M KH_2PO_4 (pH 3.5) and analyzed by autoradiography. The data were fit to a single exponential equation in GraphPad Prism5. All reactions were performed at least twice; the standard error of the curve fit for the combined replicates is reported.

Peptide-bond formation reactions

70S initiation complexes were formed as described (Miller et al. 2011). The Phe-$tRNA^{Phe}$ ternary complex was prepared by incubating 5 μM charged Phe-$tRNA^{Phe}$, 20 μM EF-Tu, and 1 mM GTP in buffer A (50 mM Tris-HCl at pH 7.5, 70 mM NH_4Cl, 30 mM KCl, 7 mM $MgCl_2$, and 1 mM dithiothreitol). The tmRNA–SmpB quaternary complexes were prepared by incubating 5 μM charged tmRNA (~10 μM total), 20 μM SmpB, and 1 mM GTP in buffer A on ice for 5 min; 20 μM EF-Tu was added, and the reaction mixture was incubated for 15 min on ice.

Peptide-bond formation rate reactions were carried out at 20°C by mixing equal volumes of initiation complexes with either ternary or quaternary complexes. Inhibition by kirromycin was performed by incubating 200 μM kirromycin with the initiation complexes before mixing with ternary or quaternary complexes. The reactions were stopped at the desired times by addition of KOH to a final concentration of 0.3 M. Reactions with relatively fast rate constants (>0.05 sec^{-1}) were performed on the KinTek RQF-3 quench-flow instrument. Reaction products were resolved using cellulose TLC plates in pyridine acetate (pH 2.8) as described (Youngman et al. 2004) and analyzed by autoradiography. The data were fit to a single exponential equation with GraphPad Prism5 software. All reported reactions were performed at least twice; the standard error of the curve fit for the combined replicates is reported.

Fluorescence measurements

$tRNA^{Phe}$ was labeled with proflavin by resuspending 100 μM $tRNA^{Phe}$ in 50 mM Tris-HCl (pH 7.5) and 10 mg/mL $NaBH_4$ (in 10 mM KOH). After incubating for 1 h at 0°C, the $tRNA^{Phe}$ was precipitated with ethanol and resuspended in 0.1 M NaOAc (pH 4.2). The $tRNA^{Phe}$ was incubated with 30 mM proflavin for 16 h at 37°C. Excess proflavin was removed by phenol:chloroform extraction followed by ethanol precipitation. The labeled $tRNA^{Phe}$ was resuspended in water and aminoacylated as described above.

Labeled ribosome complexes were assembled by incubating 2 μM 70S ribosomes; 6 μM mRNA; 3 μM fMet-$tRNA^{fMet}$; 3 μM each IF1, IF2, and IF3; and 2 mM GTP in buffer A for 45 min at 37°C. Ternary complexes containing labeled Phe-$tRNA^{Phe}$ were made by incubating 20 μM EF-Tu, 2 μM labeled Phe-$tRNA^{Phe}$, 1.6 mM GTP, and 2 μM EF-G in buffer A for 15 min on ice. The ribosome initiation complex and ternary complex were mixed and allowed to incubate for 10 min at 37°C. The labeled complex was purified by layering over a 1.3-mL sucrose cushion (1.1 M sucrose, 20 mM Tris-HCl at pH 7.5, 500 mM NH_4Cl, 10 mM $MgCl_2$, 0.5 mM EDTA) and spun at 258,000*g* in a TLA100.3 rotor for 2 h. The resulting pellet was resuspended in buffer A and stored at −80°C.

Fluorescence measurements were performed on a Fluorolog-3 spectrofluorometer (Horiba). The excitation wavelength was 449 nm. Emission spectra were obtained as SmpB at desired concentrations was added to 5 nM labeled ribosome complexes.

ACKNOWLEDGMENTS

We thank Megan McDonald-Gilmore and Kristin Smith-Koutmou for assistance with the fluorescence experiments, Daisuke Kurita and Hyouta Himeno for providing the SmpB tail peptide and valuable advice, and Rachel Green and Hani Zaher for critical reading of the manuscript. This work was supported by NIH grant GM77633.

Received August 28, 2013; accepted November 7, 2013.

REFERENCES

Andersen ES, Rosenblad MA, Larsen N, Westergaard JC, Burks J, Wower IK, Wower J, Gorodkin J, Samuelsson T, Zwieb C. 2006. The tmRDB and SRPDB resources. *Nucleic Acids Res* **34:** D163–D168.

Barends S, Wower J, Kraal B. 2000. Kinetic parameters for tmRNA binding to alanyl-tRNA synthetase and elongation factor Tu from *Escherichia coli*. *Biochemistry* **39:** 2652–2658.

Barends S, Karzai AW, Sauer RT, Wower J, Kraal B. 2001. Simultaneous and functional binding of SmpB and EF-Tu-GTP to the alanyl acceptor arm of tmRNA. *J Mol Biol* **314:** 9–21.

Bessho Y, Shibata R, Sekine S, Murayama K, Higashijima K, Hori-Takemoto C, Shirouzu M, Kuramitsu S, Yokoyama S. 2007. Structural basis for functional mimicry of long-variable-arm tRNA by transfer-messenger RNA. *Proc Natl Acad Sci* **104:** 8293–8298.

Brunelle JL, Youngman EM, Sharma D, Green R. 2006. The interaction between C75 of tRNA and the A loop of the ribosome stimulates peptidyl transferase activity. *RNA* **12:** 33–39.

Cochella L, Green R. 2005. An active role for tRNA in decoding beyond codon:anticodon pairing. *Science* **308:** 1178–1180.

Cochella L, Brunelle JL, Green R. 2007. Mutational analysis reveals two independent molecular requirements during transfer RNA selection on the ribosome. *Nat Struct Mol Biol* **14:** 30–36.

Daviter T, Gromadski KB, Rodnina MV. 2006. The ribosome's response to codon–anticodon mismatches. *Biochimie* **88:** 1001–1011.

Gromadski KB, Rodnina MV. 2004. Kinetic determinants of high-fidelity tRNA discrimination on the ribosome. *Mol Cell* **13:** 191–200.

Hallier M, Ivanova N, Rametti A, Pavlov M, Ehrenberg M, Felden B. 2004. Pre-binding of small protein B to a stalled ribosome triggers *trans*-translation. *J Biol Chem* **279:** 25978–25985.

Huang C, Wolfgang MC, Withey J, Koomey M, Friedman DI. 2000. Charged tmRNA but not tmRNA-mediated proteolysis is essential for *Neisseria gonorrhoeae* viability. *EMBO J* **19:** 1098–1107.

Hutchison CA, Peterson SN, Gill SR, Cline RT, White O, Fraser CM, Smith HO, Venter JC. 1999. Global transposon mutagenesis and a minimal *Mycoplasma* genome. *Science* **286:** 2165–2169.

Ivanova N, Pavlov MY, Felden B, Ehrenberg M. 2004. Ribosome rescue by tmRNA requires truncated mRNAs. *J Mol Biol* **338:** 33–41.

Janssen BD, Hayes CS. 2012. The tmRNA ribosome-rescue system. *Adv Protein Chem Struct Biol* **86:** 151–191.

Julio SM, Heithoff DM, Mahan MJ. 2000. *ssrA* (tmRNA) plays a role in *Salmonella enterica* serovar Typhimurium pathogenesis. *J Bacteriol* **182:** 1558–1563.

Kaur S, Gillet R, Li W, Gursky R, Frank J. 2006. Cryo-EM visualization of transfer messenger RNA with two SmpBs in a stalled ribosome. *Proc Natl Acad Sci* **103:** 16484–16489.

Kurita D, Sasaki R, Muto A, Himeno H. 2007. Interaction of SmpB with ribosome from directed hydroxyl radical probing. *Nucleic Acids Res* **35:** 7248–7255.

Kurita D, Muto A, Himeno H. 2010. Role of the C-terminal tail of SmpB in the early stage of *trans*-translation. *RNA* **16:** 980–990.

Miller MR, Liu Z, Cazier DJ, Gebhard GM, Herron SR, Zaher HS, Green R, Buskirk AR. 2011. The role of SmpB and the ribosomal decoding center in licensing tmRNA entry into stalled ribosomes. *RNA* **17:** 1727–1736.

Moore SD, Sauer RT. 2005. Ribosome rescue: tmRNA tagging activity and capacity in *Escherichia coli*. *Mol Microbiol* **58:** 456–466.

Moore SD, Sauer RT. 2007. The tmRNA system for translational surveillance and ribosome rescue. *Annu Rev Biochem* **76:** 101–124.

Neubauer C, Gillet R, Kelley AC, Ramakrishnan V. 2012. Decoding in the absence of a codon by tmRNA and SmpB in the ribosome. *Science* **335:** 1366–1369.

Nonin-Lecomte S, Germain-Amiot N, Gillet R, Hallier M, Ponchon L, Dardel F, Felden B. 2009. Ribosome hijacking: A role for small protein B during *trans*-translation. *EMBO Rep* **10:** 160–165.

Ogle JM, Ramakrishnan V. 2005. Structural insights into translational fidelity. *Annu Rev Biochem* **74:** 129–177.

Ogle JM, Brodersen DE, Clemons WM Jr, Tarry MJ, Carter AP, Ramakrishnan V. 2001. Recognition of cognate transfer RNA by the 30S ribosomal subunit. *Science* **292:** 897–902.

Ogle JM, Murphy FV, Tarry MJ, Ramakrishnan V. 2002. Selection of tRNA by the ribosome requires a transition from an open to a closed form. *Cell* **111:** 721–732.

Okan NA, Bliska JB, Karzai AW. 2006. A role for the SmpB–SsrA system in *Yersinia pseudotuberculosis* pathogenesis. *PLoS Pathog* **2:** e6.

Pape T, Wintermeyer W, Rodnina M. 1999. Induced fit in initial selection and proofreading of aminoacyl-tRNA on the ribosome. *EMBO J* **18:** 3800–3807.

Ramadoss NS, Alumasa JN, Cheng L, Wang Y, Li S, Chambers BS, Chang H, Chatterjee AK, Brinker A, Engels IH, et al. 2013. Small molecule inhibitors of *trans*-translation have broad-spectrum antibiotic activity. *Proc Natl Acad Sci* **110:** 10282–10287.

Rodnina MV, Pape T, Fricke R, Kuhn L, Wintermeyer W. 1996. Initial binding of the elongation factor Tu•GTP•aminoacyl-tRNA complex preceding codon recognition on the ribosome. *J Biol Chem* **271:** 646–652.

Rutledge LR, Campbell-Verduyn LS, Wetmore SD. 2007. Characterization of the stacking interactions between DNA or RNA nucleobases and the aromatic amino acids. *Chem Phys Lett* **444:** 167–175.

Schmeing TM, Voorhees RM, Kelley AC, Gao YG, Murphy FV, Weir JR, Ramakrishnan V. 2009. The crystal structure of the ribosome bound to EF-Tu and aminoacyl-tRNA. *Science* **326:** 688–694.

Schrader JM, Chapman SJ, Uhlenbeck OC. 2011. Tuning the affinity of aminoacyl-tRNA to elongation factor Tu for optimal decoding. *Proc Natl Acad Sci* **108:** 5215–5220.

Shimizu Y, Ueda T. 2006. SmpB triggers GTP hydrolysis of elongation factor Tu on ribosomes by compensating for the lack of codon–anticodon interaction during *trans*-translation initiation. *J Biol Chem* **281:** 15987–15996.

Shimizu Y, Inoue A, Tomari Y, Suzuki T, Yokogawa T, Nishikawa K, Ueda T. 2001. Cell-free translation reconstituted with purified components. *Nat Biotechnol* **19:** 751–755.

Sundermeier TR, Dulebohn DP, Cho HJ, Karzai AW. 2005. A previously uncharacterized role for small protein B (SmpB) in transfer messenger RNA-mediated *trans*-translation. *Proc Natl Acad Sci* **102:** 2316–2321.

Thibonnier M, Thiberge JM, De Reuse H. 2008. *Trans*-translation in *Helicobacter pylori*: Essentiality of ribosome rescue and requirement of protein tagging for stress resistance and competence. *PLoS ONE* **3:** e3810.

Valle M, Gillet R, Kaur S, Henne A, Ramakrishnan V, Frank J. 2003. Visualizing tmRNA entry into a stalled ribosome. *Science* **300:** 127–130.

Vogeley L, Palm GJ, Mesters JR, Hilgenfeld R. 2001. Conformational change of elongation factor Tu (EF-Tu) induced by antibiotic binding. Crystal structure of the complex between EF-Tu·GDP and aurodox. *J Biol Chem* **276:** 17149–17155.

Walker SE, Fredrick K. 2008. Preparation and evaluation of acylated tRNAs. *Methods* **44:** 81–86.

Youngman EM, Green R. 2005. Affinity purification of in vivo-assembled ribosomes for in vitro biochemical analysis. *Methods* **36:** 305–312.

Youngman EM, Brunelle JL, Kochaniak AB, Green R. 2004. The active site of the ribosome is composed of two layers of conserved nucleotides with distinct roles in peptide bond formation and peptide release. *Cell* **117:** 589–599.

Zaher HS, Green R. 2009. Fidelity at the molecular level: Lessons from protein synthesis. *Cell* **136:** 746–762.